29th EPS Conference on Plasma Phys. and Contr. Fusion Montreux, 17-21 June 2002 ECA Vol. **26B**, O-4.01 (2002)

Drift kinetic simulations of the current driving the necolassical tearing mode

E. Poli, A. G. Peeters, A. Bergmann, S. Günter, S. D. Pinches

Max-Planck-Institut für Plasmaphysik, EURATOM Association,
D-85748 Garching, Germany

Neoclassical tearing modes (NTMs) pose a serious limitation to the achievable energy content of a toroidally confined plasma and the prediction of their behaviour in a fusion reactor is an important open issue. The description of the NTM is usually given in terms of the generalized Rutherford equation, which is a time-evolution equation for the half-width of the island W [1-5]:

$$\frac{dW}{dt} = c_1\Delta' + \frac{c_2}{W}\int_{-1}^{\infty} d\Omega \oint \frac{d\xi \cos\xi}{\sqrt{\cos\xi + \Omega}}\, j_{\|}^{n.i.}. \qquad (1)$$

In the previous equation, the helical angle $\xi \equiv m\theta - n\varphi$, where m and n are the poloidal and toroidal number of the resonant rational surface and θ and φ are the poloidal and toroidal angles, has been introduced along with the helical flux $\Omega \equiv (q_s'/2q_s)(\psi - \psi_s)^2/\tilde{\psi} - \cos\xi$, where ψ is the unperturbed poloidal flux, the prime denotes the derivative with respect to ψ, $\tilde{\psi}$ is the strength of the flux perturbation and the subscript s means that a quantity is evaluted at the resonant surface. The helical flux Ω is used as a label of the perturbed magnetic surfaces. The first term on the right-hand side of Eq.(1) expresses the contribution of the equilibrium current profile (which is usually supposed to be stabilizing), whereas the second term is connected with the current perturbation due to the presence of the island itself. In this paper, two contributions to the perturbed current $j_{\|}^{n.i.}$ entering Eq. (1) are considered. The first one is related with the bootstrap current perturbation in the presence of the island: inside the reconnected region, due to the high parallel transport along the field lines the pressure is flattened and the bootstrap current (which is proportional to the pressure gradient) drops. This current perturbation leads for conventional positive shear to a further growth of the initial magnetic perturbation and drives it unstable. The second contribution to $j_{\|}^{n.i.}$ addressed in this paper is connected with the time-dependent potential associated with the motion of the island with respect to the surrounding plasma. The polarization current which arises from this potential is also predicted to play a role (whether stabilizing or destabilizing is not known) in the island evolution described by Eq. (1). In the standard analytic theory, the perturbed current $j_{\|}^{n.i.}$ is calculated from the drift kinetic equation (or the neoclassical fluid equations) employing a double expansion in the small parameters w_b/W, W/r_s, where w_b is the ion banana width and r_s the minor radius of the resonant surface. However, the first condition is not always verified in the experiments. At ASDEX Upgrade (AUG), for instance, the width of the seed island which triggers the mode is between 1 and 5 cm, whilst the width of a banana orbit is between 7 mm and 3 cm, so that

the limit $w_b \approx W$ (which will be called the "small island" limit) is crucial at least in the early phase of the mode, and hence for the onset criteria. In the limit of small island widths, it can be thought that the trapped ions flowing in the island region can overlap it significantly, and hence smear out the effects connected with the different behaviour of the plasma inside and outside the island. Such an effect is of course of no importance for the electrons, that have a much narrower banana width (i.e. negligible overlap with the island). In order to investigate these effects, a numerical solution of the drift kinetic equation in toroidal geometry in the presence of an island is needed.

The drift kinetic equation

$$\frac{df}{dt} = \frac{\partial f}{\partial t} + \left(v_{\|}\hat{\mathbf{b}} + \mathbf{v}_d\right)\cdot\frac{\partial f}{\partial \mathbf{r}} - \frac{e}{m_i}\nabla\Phi\cdot\frac{\partial f}{\partial \mathbf{v}} = C(f) \tag{2}$$

is solved by employing the δf method. In Eq.(2), $\hat{\mathbf{b}}$ is a unit vector along the magnetic field, $v_{\|}$ and $\mathbf{v}_d$ are the parallel and magnetic drift velocity of the guiding center, respectively, e is the ion charge, m_i the ion mass and Φ the potential. In the δf method, the distribution function is split into a an analytic time-independent part f_0 (taken to be a Maxwellian f_M here) and a part which is represented by the distribution in the phase space of a set of markers, that represent the ions (as it has been mentioned above, the effects connected with a small island are unrelevant for electrons). The markers evolve according to a set of Hamiltonian equations of motion, which are integrated using the HAGIS code [6]. Collisions are implemented by means of a Monte Carlo procedure [7].

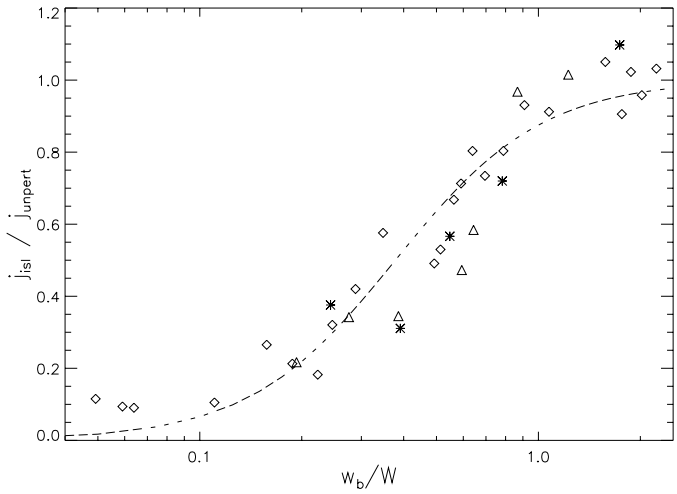

Fig. 1. Averaged current density inside the island versus the ratio w_b/W . Simulations are performed with ITER-like parameters (diamonds), and AUG parameters with both deuterium plasma (stars) and hydrogene plasma (triangles)

Eq. (2) has been applied to the study of bootstrap and polarization current. In the first case, the potential Φ is switched off, the island is kept at a fixed position and the equilibrium temperature and density profiles are prescribed analytically. The results of the simulations show that the bootstrap current drops to zero inside a large island, as it is expected in the standard

theory. In the limit of a small island, $w_b \approx W$, the trapped particles that overlap the island are able to restore the full parallel ion flux inside it (Fig. 1). In other words, in this limit the ion drive of the NTM vanishes and the island is mainly driven by the electrons. Moreover, this process leads to a scaling condition for β_p (the ratio of the plasma to the poloidal magnetic energy) at the onset of the mode which is linear in the normalized poloidal ion gyroradius ρ^*_{pi}, in agreement with the experimental observation at ASDEX Upgrade. These results have been published in Ref. 8.

The focus in this paper is mainly on the simulations of the polarization current. This current arises from the relative motion of the island with respect to the plasma. In this paper, the reference frame is assumed where the island is fixed and the plasma flows around it.

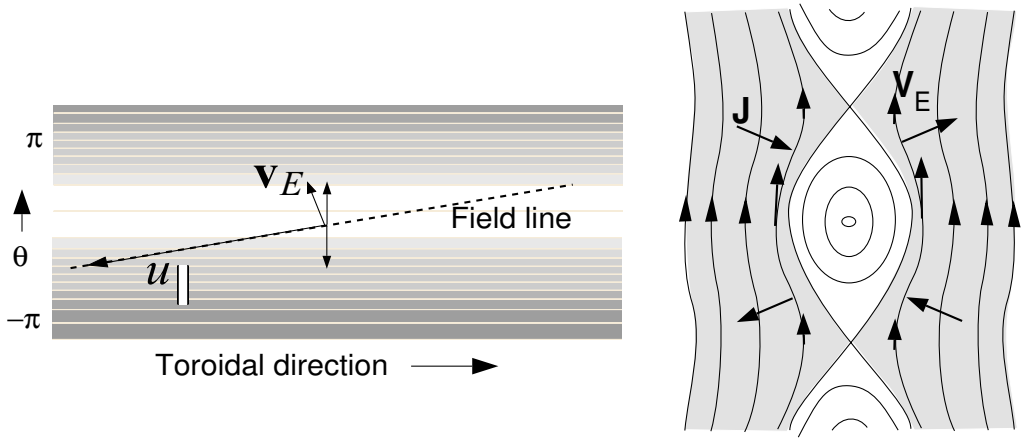

Fig. 2. a*: Generation of the parallel flow* $u_{||}$. b*: Orientation of the polarization current.*

The potential associated with the island [4,5] is in this case a flux surface quantity (i.e. the electric field E_r is perpendicular to the perturbed flux surfaces) and vanishes inside the island. Due to the damping of the poloidal rotation, the plasma develops a large parallel flow $u_{||} = cE_r/B_p$ (B_p is the poloidal magnetic field) such that its poloidal component compensates the poloidal component of the $\mathbf{E}\times\mathbf{B}$ velocity $\mathbf{v}_E$ (Fig. 2a). Since at least the contribution of the trapped particles to this parallel flow is not constant along the perturbed magnetic surfaces, there is a (parallel) inertial force that accelerates the plasma at some positions along the flux surface and decelerates it at other positions. This inertial force is balanced by the Lorentz force $\mathbf{j}\times\mathbf{B}$, generated by a radial current which is the polarization current (Fig. 2b). It can be expressed as

$$j_{\mathrm{pol}} = en/\omega_{cp}\,(\mathbf{v}_E\cdot\nabla)\,u_{||}, \tag{3}$$

where n is the density and ω_{cp} is the cyclotron frequency calculated with the poloidal field. Since the electron cyclotron frequency is much larger than the ion cylclotron frequency, it turns out that the polarization current is carried mostly by the ions.

These parallel and radial fluxes are simulated employing the numerical scheme outlined above. In this case, the equilibrium pressure is uniform (no gradient) and the electric potential is prescribed analytically. The simulated parallel flux is found to coincide with $u_{||}$. The radial

profile of the simulated polarization current is shown in Fig. 3, where the two curves show the flux-surface averages of the perpendicular fluxes in the upper and lower part of the island. The two contribution are equal in magnitude and have opposite sign, in agreement with the picture given above (cf. Fig. 2b). It has also been found that the simulated polarization current scales quadratically with the plasma rotation frequency ω, in agreement with Eq. (3) and with the fact that $\Phi \propto \omega$.

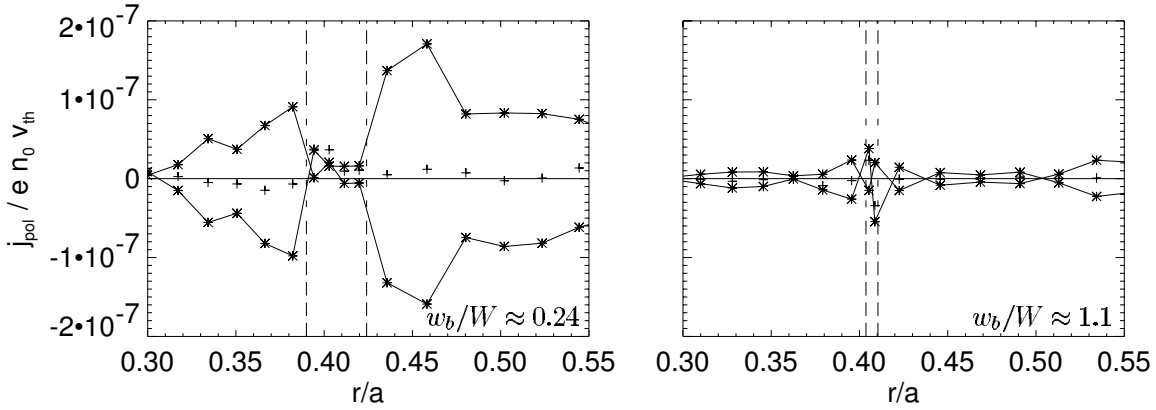

Fig. 3. Polarization current in the presence of a large (a) *and small* (b) *island*

The only parameter which has been changed in Fig. 3b with respect to Fig. 3a is the island width. It can be seen that in the limit $w_b \approx W$ the polarization current is strongly reduced. This effect is not predicted in the standard analytic theory, which can not be applied for $W \approx w_b$. However, this is the range where the polarization current is usually believed to play a role in determining the threshold for the NTM. A further investigation is needed in order to make a more quantitative estimate of the influence of the small-island limit on the threshold model.

References

1) P. H. Rutherford, Phys. Fluids **16**, 1903 (1973).
2) R. Carrera, R. D. Hazeltine, M. Kotschenreuther, Phys. Fluids **29**, 899 (1986).
3) W. X. Qu, J. D. Callen, University of Wisconsin Plasma Report No. UWPR 85-5 (1985).
4) A. I. Smolyakov et al., Phys. Plasmas **2**, 1581 (1995).
5) H. R. Wilson, J. W. Connor, R. J. Hastie, C. C. Hegna, Phys. Plasmas **3**, 248 (1996).
6) S. D. Pinches et al., Comp. Phys. Comm. **111**, 133 (1998).
7) A. Bergmann, A. G. Peeters, S. D. Pinches, Phys. Plasmas **8**, 5192 (2001).
8) E. Poli et al., Phys. Rev. Letters **88**, 075001 (2002).